Fiber Diffraction from Filamentous Plant Viruses

G. Stubbs, A. Kendall
Vanderbilt University, Nashville, TN, U.S.A.

Introduction

Filamentous macromolecular assemblies are of great importance in biology. However, many of these structures (e.g., the filamentous components of animal and human viruses such as HIV and influenza) are labile and difficult to study structurally. The filamentous plant viruses are exceptions and have been invaluable as both structural models and model systems for methodological development.

The potexviruses are flexible filamentous viruses, important not only as model systems but also in their own right. Potato virus X (PVX) and papaya mosaic virus (PMV) are the best-studied members of the genus, and PVX, the type member, is of considerable significance to both biotechnology [1] and agriculture [2]. Early fiber diffraction studies [3, 4] had shown that it has a helical structure, with just under nine subunits per helical turn. Diffraction patterns were not, however, sufficiently well ordered to obtain more information than this. To realize the full potential of PVX as a model system and in biotechnology, many more details about the subunit structure and therefore much better diffraction patterns are required.

The rigid tobamoviruses have been much more fully characterized structurally than any other filamentous viruses. The structures of tobacco mosaic virus (TMV) [5], the U2 strain of tobacco mosaic virus [6], cucumber green mottle mosaic virus [7], and ribgrass mosaic virus [8] have been determined by fiber diffraction methods at resolutions between 2.9 and 3.5 Å. Because they can be studied at high resolution, tobamoviruses have a unique role as model systems for filamentous biological assemblies, and it is therefore desirable to obtain the best possible structural data for them. Our current tobamovirus studies focus on odontoglossum ringspot virus (ORSV), because we have found that this virus forms excellent specimens for x-ray fiber diffraction and because of its value in studies of viral host specificity [9].

Methods and Materials

PVX was purified from infected tobacco plants (*N. clevelandii*) by a modification of the method of Shepard [10, 11]. PMV was purified from infected papaya trees by a modification of the method of Erickson and Bancroft [12]. Modifications included the use of protease inhibitors. ORSV was a gift from W. O. Dawson.

Oriented sols for fiber diffraction were prepared from the two potexviruses by drawing material from soft centrifuged virus pellets into thin-walled glass capillaries, centrifuging the capillaries slowly for several days, removing the dilute upper portions of the samples, and exposing the samples to high magnetic fields (up 18.8 T) for days to weeks [11, 13]. Oriented sols of ORSV were prepared by the shearing method of Gregory and Holmes [14].

Fiber diffraction data were collected at the Bio-CAT beamline of the APS. The specimens were mounted with the fiber axis being vertical. The beam had dimensions of 35 μm vertically and 60 μm horizontally at the detector, and it was very close to this size at the specimen. Data were recorded by using a charged-coupled device (CCD) detector approximately 100 mm from the specimen. The detector measured approximately 85 mm horizontally and 50 mm vertically, with an effective pixel size of 24 μm^2 (the actual pixel size was 12 μm^2, but pixels were binned in 2×2 arrays). The x-ray wavelength was 1.03 Å.

Data were analyzed by using the public domain NIH Image program (developed at the U.S. National Institutes of Health, http://rsb.info.nih.gov/nih-image) for direct measurements and the program WCEN (H. Wang and G. Stubbs, unpublished) for measurements in reciprocal space, including the fitting of layer lines.

Results

A diffraction pattern from the best oriented PVX sol is shown in Fig. 1. The mean disorientation (deviation of the particle axis from the filament axis) is between 4° and 5°. This sol is not as well oriented as the best sols of TMV, which achieve disorientations of 1° or less. It is, however, much better oriented than any previously oriented flexible filamentous virus.

The pattern is characterized by a series of near-meridional layer lines spaced $1/34.5$ $Å^{-1}$ apart, demonstrating a viral helix pitch of 34.5 ± 0.5 Å, in good agreement with the previously determined value [3] of 34.3 Å. Unlike previously recorded patterns, however, the pattern also shows diffraction maxima away from the near-meridional layer lines. In particular, very strong off-equatorial intensity is seen near the center of the pattern. In previously reported PVX diffraction patterns, this intensity could not be distinguished from the equator. In the pattern shown in Fig. 1, however, it clearly belongs to the first layer line.

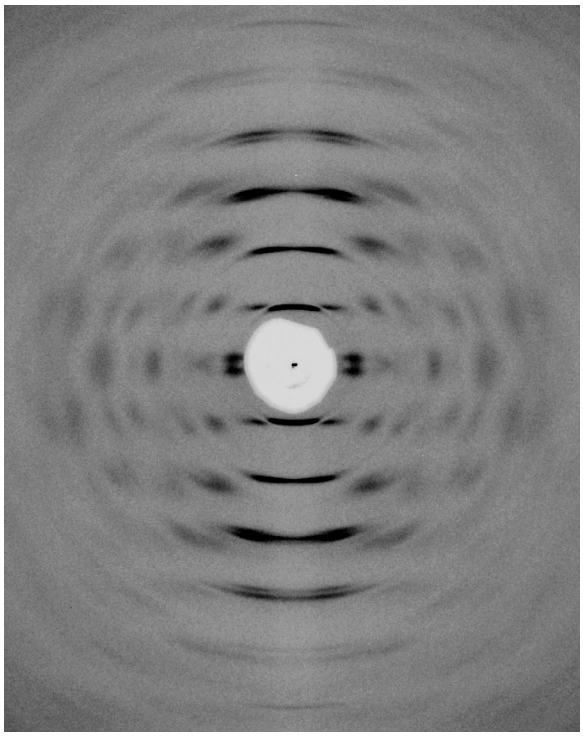

FIG. 1. Diffraction pattern from PVX.

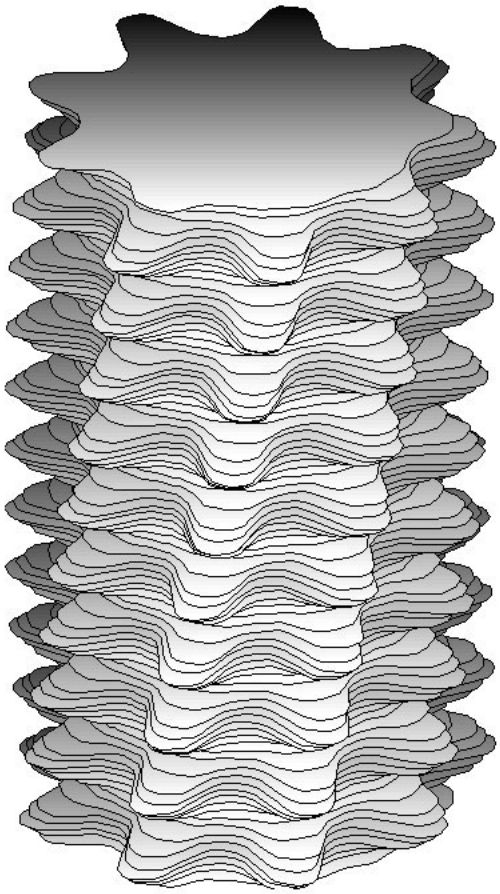

FIG. 2. Schematic drawing of a segment of PVX. Two sets of grooves are seen: One set is almost longitudinal, while the other follows the viral helix.

An excellent fit of layer lines to the diffracted intensity was obtained visually by using a layer line spacing of 1/345 $Å^{-1}$. This fit was made possible by the presence of the clearly defined first layer line. The first near-meridional layer line, at 1/34.5 $Å^{-1}$, is, in fact, the tenth layer line rather than the eighth, as previously suggested by electron microscopic observations [3, 15]. In other words, the viral helix repeats exactly or almost exactly in 10 turns. Our results therefore show that there are 8.90 ± 0.01 subunits per turn of the viral helix.

Analysis of the PVX diffraction pattern [11] showed that the viral surface is characterized by intersecting sets of deep grooves, with one set running almost longitudinally and the other following the simple viral helix (Fig. 2).

A series of excellent fiber diffraction patterns was obtained from the ORSV specimens (Fig. 3). Although not yet analyzed, these patterns contain excellent data at resolutions of better than 2.8 Å.

Discussion

The surprising observation that the diffracted intensity previously attributed to the equator in PVX is actually from the first layer line was made possible only by the combination of improved orientation and the very small x-ray beam obtainable at the Bio-CAT synchrotron facility. The first layer line shows that the surface of PVX is much more deeply grooved than, for example, the surface of the rigid rod TMV; the grooves presumably make a major contribution to the flexibility of PVX and, by analogy, to the flexibility of the other potexviruses.

The patterns obtained here will allow the structural determination of these viruses at resolutions higher than any that have previously been possible. The potexvirus patterns (including those of PMV, not shown) should allow analysis to 6-Å resolution, although some sort of model will be required. Such a model could, in theory, be obtained from a crystallographic analysis of the isolated coat protein fragment of the virus [16] or from cryoelectron microscopy. The ORSV pattern is sufficiently good to allow analysis at 2.8-Å resolution or better without input from any other experimental technique. It should be possible to refine a model obtained from a lower-resolution analysis [17] against these data.

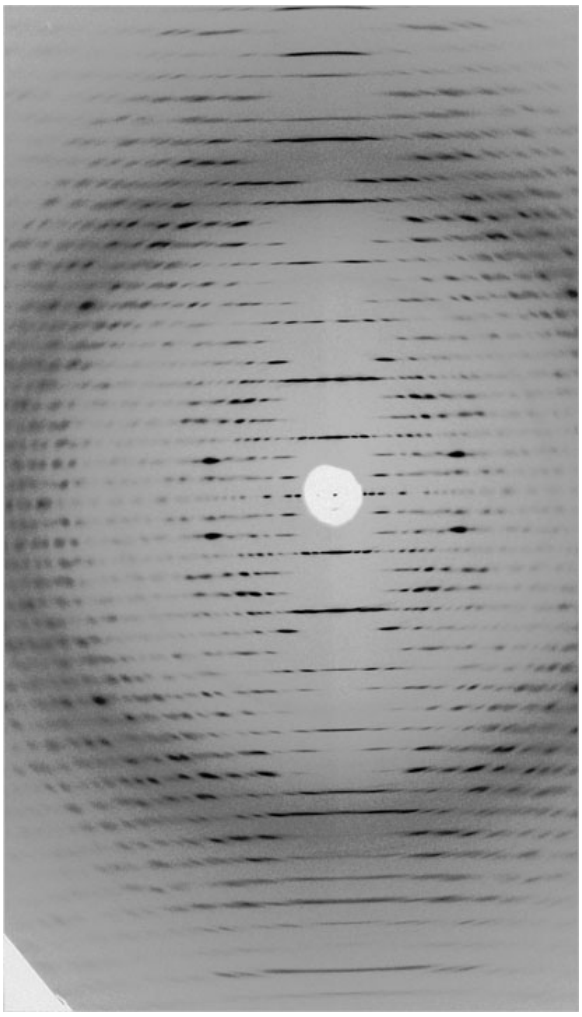

FIG. 3. Diffraction pattern from ORSV.

Acknowledgments

This work was supported by Grant Nos. MCB-9809879, MCB-9942600, DBI-9604789, and INT-9602486 from the National Science Foundation. Use of the APS was supported by the U.S. Department of Energy, Office of Science, Office of Basic Energy Sciences, under Contract No. W-31-109-ENG-38. Bio-CAT is a National Institutes of Health-supported Research Center RR-08630.

References

[1] S. Santa Cruz, S. Chapman, A.G. Roberts, I. M. Roberts, D. A. M. Prior, and K. J. Oparka, Proc. Natl. Acad. Sci. U.S.A. **93**, 6286-6290 (1996).

[2] K. A. White, M. Rouleau, J. B. Bancroft, and G. A. Mackie, in *Encyclopedia of Virology*, edited by R. G. Webster and A. Ganoff (Academic Press, London, England, 1994), Vol. 2, pp. 1142-1147.

[3] P. Tollin, H. R. Wilson, and J. B. Bancroft, J. Gen. Virol. **49**, 407-410 (1980).

[4] G. Stubbs, G. Ferrell, M. Reams, and N. Fletcher, Fibre Diffraction Rev. **9**, 24-28 (2000).

[5] K. Namba, R. Pattanayek, and G. Stubbs, J. Mol. Biol. **208**, 307-325 (1989).

[6] R. Pattanayek and G. Stubbs, J. Mol. Biol. **238**, 516-528 (1992).

[7] H. Wang and G. Stubbs, J. Mol. Biol. **239**, 371-384 (1994).

[8] H. Wang, J. N. Culver, and G. Stubbs, J. Mol. Biol. **269**, 769-779 (1997).

[9] M. E. Hilf, W. O. Dawson, Virology **193**, 106-114 (1993).

[10] J. F. Shepard, Bulletin 662 of the Montana Agricultural Experimental Station (1972).

[11] L. Parker, A. Kendall, and G. Stubbs, in Virology (in press, 2002).

[12] J. W. Erickson and J. B. Bancroft, Virology **90**, 36-46 (1978).

[13] I. Yamashita, H. Suzuki, and K. Namba, J. Mol. Biol. **278**, 609-615 (1998).

[14] J. Gregory and K.C. Holmes, J. Mol. Biol. **13**, 796-801 (1965).

[15] R. W. Horne, J. M Hobart, and I. P. Ronchetti, Micron **5**, 233-261 (1975).

[16] C. Bunick, A. C. T. North, and G. Stubbs, Acta Crystallogr. D **56**, 1430-1431 (2000).

[17] H. Wang, A. Planchart, and G. Stubbs, Biophys. J. **74**, 633-638 (1998).